IEEE Robotics and Automation Letters (RAL) paper presented at the
2020 IEEE/RSJ International Conference on Intelligent Robots and Systems (IROS)
October 25-29, 2020, Las Vegas, NV, USA (Virtual)

Self-Propelled Colonoscopy Robot using Flexible Paddles*

Keisuke Osawa, Ryu Nakadate, Jumpei Arata, Yoshihiro Nagao, Tomohiko Akahoshi, Masatoshi Eto, and Makoto Hashizume

***Abstract*—The number of patients suffering from colorectal cancer (CRC) has been increasing. CRC is known to be curable if detected and treated early. Colonoscopy is currently one of the best screening methods for CRC because it can observe and treat disorders in the large intestine. However, operating the colonoscope is technically demanding for doctors because the insertion of the instrument into the large intestine requires considerable training and skill. To address this issue, we propose a novel self-propelled robot with flexible paddles for the intestinal tract. In this device, the torque is transmitted from a motor outside the patient body to a worm gear at the tip of the colonoscope by a flexible shaft. The worm gear is engaged with two spur gears, and flexible paddles fixed to these spur gears contact the wall of the large intestine to provide the propulsive force. We constructed a force transmission model of the robot to confirm the suitability of the design. The prototype of the self-propelled robot was fabricated by a 3D printer, and its locomotion in a simulated rubber intestine was evaluated. The velocity of the robot was faster than the required speed of 6.5 mm/s. The propulsive force was approximately 1 N; thus, the effectiveness of the robotic principle was confirmed. The mechanical locomotion design, its fabrication, and analysis results are reported in this paper.**

***Index Terms*—Modeling, Control, and Learning for Soft Robots, Medical Robots and Systems, Flexible robots**

I. Introduction

In recent years, the number of patients suffering from colorectal cancer (CRC) has been increasing owing to changes in diet and lifestyle and growing aged population in the society. CRC is known to be completely curable if detected and treated in the early stage [1]. Colonoscopy is the most commonly used examination method for CRC; other methods include blood test, fecal occult blood test, and CT colonography. The tip of the colonoscope is equipped with a camera, light, lens-cleaning nozzle, and forceps port. Instruments such as forceps are inserted through the forceps port, if necessary, for diagnosis and treatment. Although colonoscopy facilitates effective inspection and treatment, the insertion operation into the large intestine demands considerable skill of the physician. Insufficient skill may lengthen the duration of inspection and make the process more painful for the patient. An advanced technique is required for the insertion because the large intestinal duct is extended and contracted by an external force. Even when the colonoscope is pushed from outside of the body, the large intestine is extended and the tip of the colonoscope does not advance. Furthermore, it is difficult to insert the colonoscope into the sigmoid colon because of the complexity of the structure (Fig. 1).

To solve this problem, capsule colonoscopes [2]-[5] and self-propelled robots [6]-[11] have been studied. The capsule endoscope has a diameter of approximately 11 mm and length of 26 mm. Therefore, it can be swallowed from the mouth for taking pictures of the digestive organs, mainly the small intestine, painlessly [2][3]. One of the biggest limitations of the capsule endoscope is that the capsule does not propel itself; therefore, it is impossible to inspect a particular area of interest. Capsule endoscopes with an active fin [4] and magnetic control from outside the body [5] were proposed to overcome this limitation. However, capsule endoscopes are used only for observation and cannot treat or perform biopsy of a lesion. Furthermore, there is a risk that the capsule is trapped in the digestive tract and cannot be discharged. Because of these problems, a tube-type colonoscope continues to be the golden standard in clinics for CRC inspection.

There have been many researches on self-propelled endoscope robots for both industrial and medical applications. A helix-type robot [6][7] can contact the wall of the large intestine while rotating a helical protrusion provided around

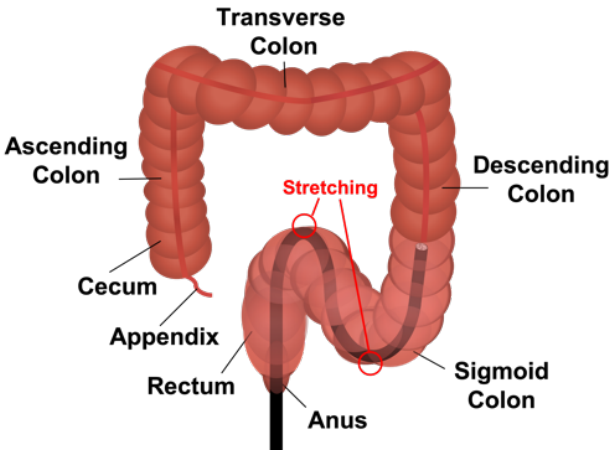

Fig. 1. Typically performed colon inspection by colonoscopy.

*Research supported by JSPS KAKENHI Grant Number JP18H03549.

Keisuke Osawa and Jumpei Arata are with the Department of Mechanical Engineering, Faculty of Engineering, Kyushu University, Fukuoka, Japan (e-mail: osawa@system.mech.kyushu-u.ac.jp).

Ryu Nakadate is with the Center for Advanced Medical Innovation, Kyushu University, Fukuoka, Japan.

Yoshihiro Nagao is with the Department of Advanced Medicine and Innovative Technology, Kyushu University Hospital, Fukuoka, Japan.

Tomohiko Akahoshi is with the Department of Advanced Medical Initiatives, Graduate School of Medical Science, Kyushu University, Fukuoka, Japan.

Masatoshi Eto is with the Department of Urology, Graduate School of Medical Sciences, Kyushu University, Fukuoka, Japan.

Makoto Hashizume is with the Kitakyushu Koga Hospital, Fukuoka, Japan.

the long axis of the flexible colonoscope to obtain the propulsive force. The device proposed in [6] has the drawback that the circumscribed circle diameter is fixed, which may cause insufficient propulsion force owing to loose contact between the robot and the intestine. The device proposed in [7] can change the diameter of the robot by making a spiral projection on the surface of the balloon, but the change in diameter is limited. The snake-type robot [8] bends at not only the tip but also the entire inserted part. It has 16 bending sections so that the sheath of the rear part automatically follows the same trajectory as the tip. However, there is a problem of cost versus benefit considering the number of wires and motors required for the robot. The inchworm-type robots [9] are provided with parts to attach to the intestinal wall; these parts can be fixed and released at both ends of a stretchable and contractible section. The principle has been commercialized as a double balloon endoscope [10]. However, it has low propulsive speed because the fixation and release steps are repeated frequently. Paddle-type robots [11] advance with the paddles pushing against the colon. However, there is a risk of damage to the colonic mucosa because of the rigid paddles.

In this study, we propose a new mechanism to propel the colonoscope through the intestine tract by rotating a flexible paddle using a worm gear mechanism. In this method, torque is transmitted from the motor outside the body to the worm gear through the flexible shaft. At the tip, two spur gears are engaged with a worm gear, and the flexible paddle fixed to these spur gears contacts the wall of the large intestine to obtain the propulsive force. This paper reports the details of the proposed method, its drive characteristics, and its evaluation.

II. DESIGN AND MODELING

A. Requirements

To develop a highly locomotive, safely self-propelled colonoscopy robot, it is necessary to understand the structure of the human colon. The general human large intestine is a continuous tube that is approximately 1.5-m long and 7.5-cm in diameter when it is inflated [12]. The human large intestine consists of six segments—rectum, sigmoid colon, descending colon, transverse colon, ascending colon, and cecum. Their average diameters are 3.6 cm, 2.6 cm, 3.3 cm, 3.7 cm, 4.5 cm, and 4.4 cm, respectively [13]. During colonoscopy, it is particularly difficult to insert the colonoscope into the sigmoid colon, which requires highly trained techniques. While inserting the colonoscope, a force is applied to the bent section of the colon, and the colonoscope is inserted while stretching the intestine, causing pain (Fig. 1). However, if there is a device that self-propels and pulls at the tip of the colonoscope instead of pushing the proximal end of the colonoscope, it is possible to insert a colonoscope deep into the large intestine without causing pain. We determined the requirements by extracting the size, expansion range, speed, and thrust force of this robot from [14]-[18], as shown in Table 1. The robot should have a diameter of ≤26 mm and length of ≤40 mm. Because the size and shape of the colon varies considerably among the patients, these values are the best estimates based on the anatomy and available literature [17]. The robot must cope with changes in the inner diameter of the large intestine to obtain a propulsive force. A linear speed of 6.5 mm/s was calculated, by assuming that an experienced colonoscopist requires 3.8 min to traverse through the colon and reach the cecum [16]. A propulsive force of ≥1 N is required for the robot to propel its own sheath while pulling it [15].

TABLE I

Specifications of the robot according to the structure of the large intestine.

Requirement	Specification
Size	Diameter of ≤26 mm [15]–[17].
	Length of ≤40 mm [15]–[17].
Expansion range	Adapt to diameters ranging from ca. 26 to 44–62 mm [16][17].
Speed	A linear speed of ≥6.5 mm/s [18].
Thrust force	A thrust force of ≥1 N [15][17].

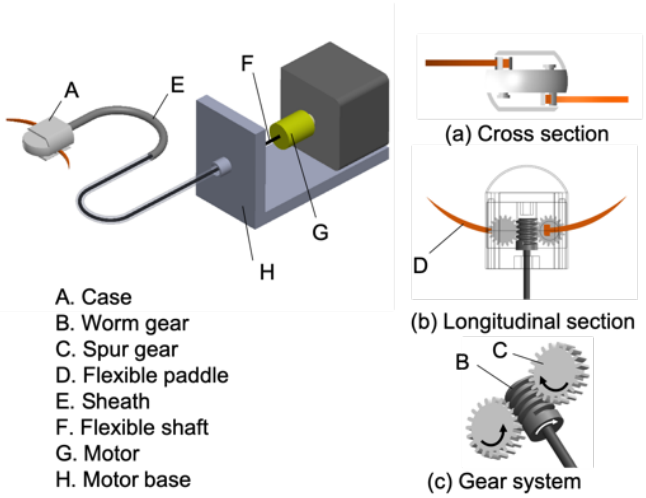

Fig. 2. Overview of the proposed self-propelled robot.

B. Structure and Locomotion Principle

The robotic structure comprises a case, worm gear, two spur gears, two flexible paddles, a sheath, a flexible shaft, and an electric motor, as shown in Fig. 2. In the proposed mechanism, torque is transmitted from the motor outside the body to the worm gear through the flexible shaft. The two spur gears are engaged with the worm gear. The flexible paddle fixed to these spur gears contacts the wall of the large intestine to obtain the propulsive force (Fig. 3). The case of the robot was carefully designed such that it does not interfere with the opposite intestinal wall by pressing the flexible paddle against the case, as shown in Fig. 2(a). Therefore, for the flexible paddle, we must select a material with flexibility capable of withstanding repeated bending deformation and elastic force that generates a propulsive force. Therefore, we considered the flexible rubber. Because the flexible paddles push against the intestinal walls by elastic force to obtain the normal force, it can navigate through the different diameters of the large intestine. In comparison with the mechanisms of other self-propelled robots [6]-[9], this robot has simpler structure and

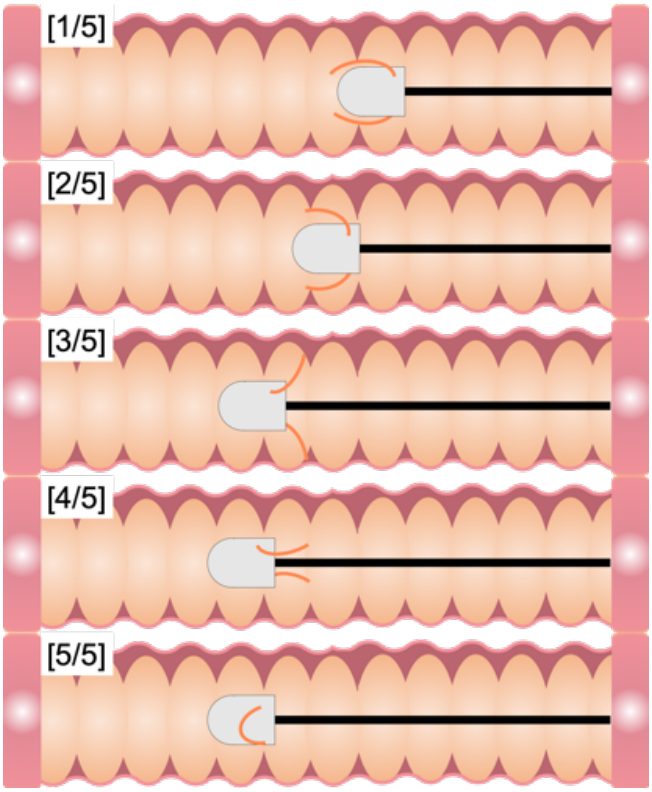

Fig. 3. Working principle of the proposed self-propelled colonoscope.

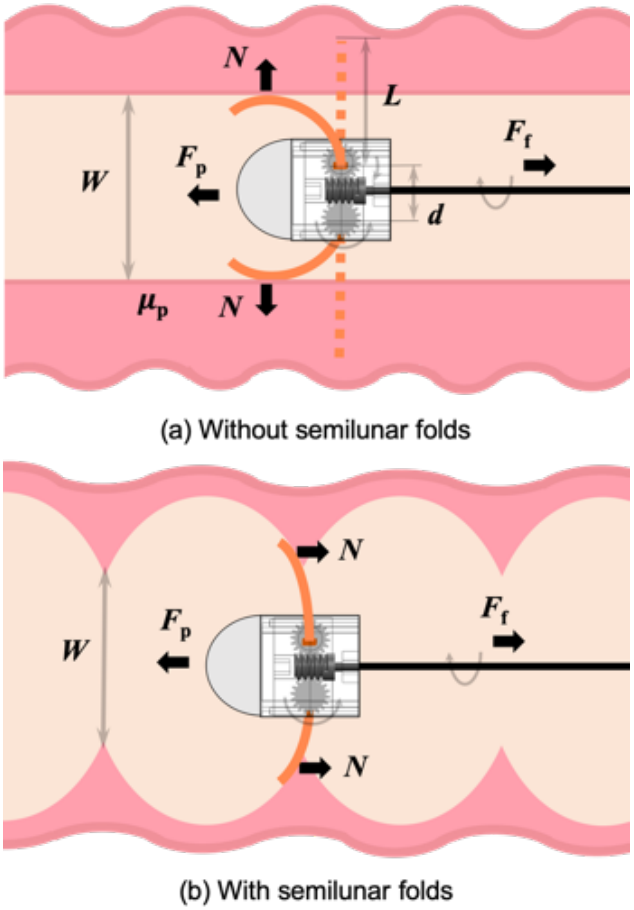

Fig. 4. Force-transmission model.

mechanism. The notable feature of the proposed mechanism is that the number of mechanical components is considerably reduced because of the use of elastic paddles. This significantly contributes to the downsizing of the device.

C. *Force-Transmission Modeling*

Fig. 4 presents the force-transmission modeling of the colonoscopy robot using the force balance equation, which allows the robot to propel forward through the large intestine. Normal force N applied to the colon wall by the flexible paddles varies depending on displacement x. N can be expressed as follows:

$$N = N(x)\ ,\ x = L - (W - d) / 2\ ,\ 0 \leqq x \leqq L \qquad (1)$$

where L is the length of the flexible paddle, W is the diameter of the lumen, and d is the center-to-center distance between two spur gears. As shown in Fig. 4(a), the proposed robot obtains the propulsive force F_p by friction against the large intestine wall, generated by the normal force N that the paddles receive from the large intestine wall. Then, F_p can be expressed as follows:

$$F_p = 2\mu_p N(x) - F_f \qquad (2)$$

Where μ_p is the dynamic frictional coefficient between the large intestinal wall and the flexible paddle, and F_f is the frictional force between the large intestine wall and sheath. In another case shown in Fig. 4(b), the reaction force generated by the normal force when the paddles push the semilunar fold of the colon is the propulsive force. Then, W is the diameter of the tip of the semilunar fold. F_p can be expressed as follows:

$$F_p = 2N(x) - F_f \qquad (3)$$

Note that the robot advances forward when F_p is a positive value.

TABLE II

Specifications of a fabricated robot.

Parameter	Dimension
Case width [mm]	26
Case length [mm]	40
Flexible paddle diameter [mm]	2 (tip) - 3.5 (proximal)
Flexible paddle length [mm]	30
Worm gear diameter [mm]	6
Spur gear diameter [mm]	9
Number of teeth of spur gear	18

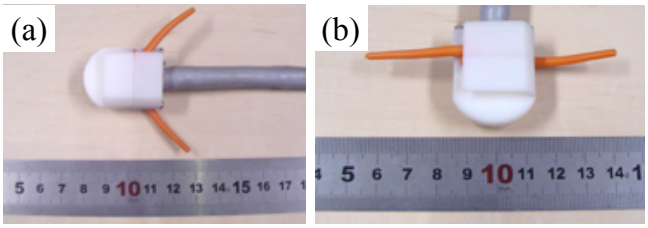

Fig. 5. Overview of the assembled self-propelled robot. (a) side view, (b) front view.

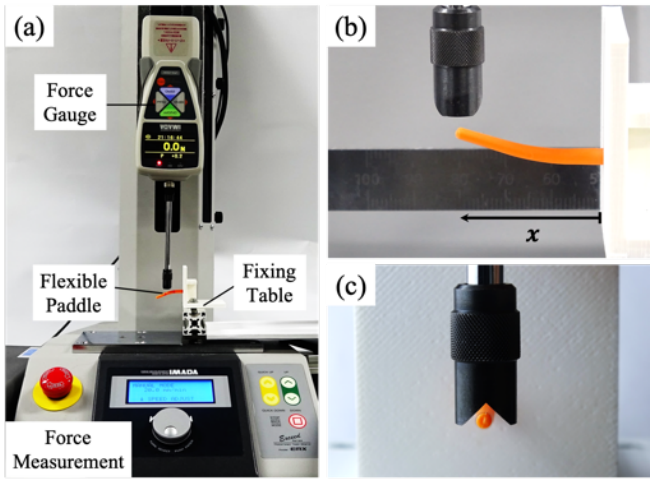

Fig. 6. (a) Experimental system of force measurement, (b) front view of the experimental system, (c) side view of the experimental system.

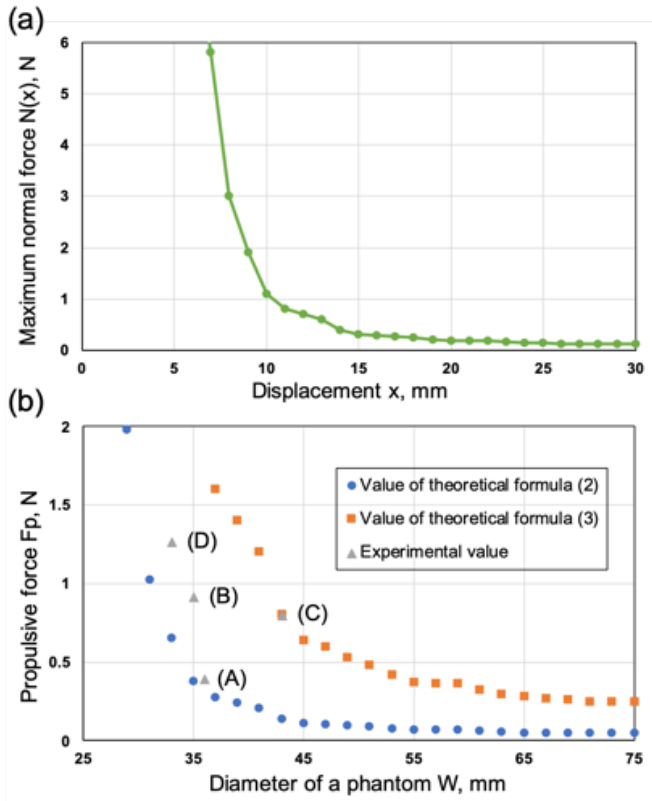

Fig. 7. Theoretical results and experimental results. (a) Maximum normal force of the flexible paddle at each displacement. (b) Propulsive force at each diameter of a phantom.

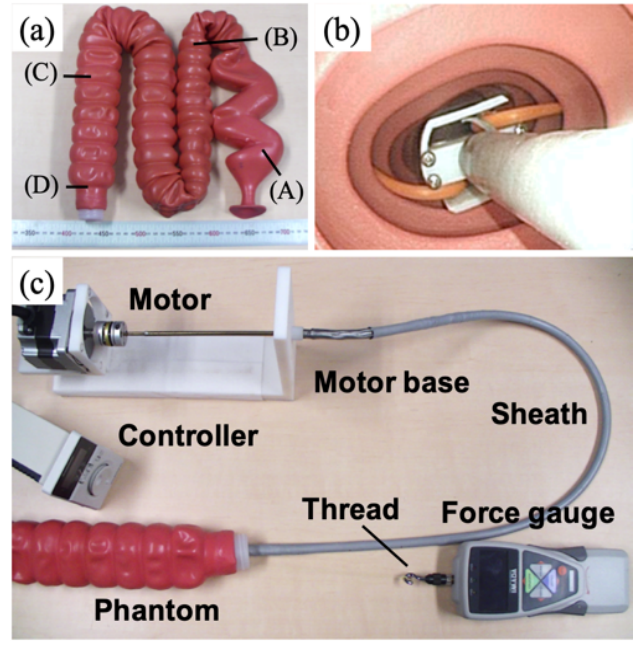

Fig. 8. (a) Colonoscopy training model; (b) locomotion in the phantom and (c) experimental setup.

III. Evaluations and Discussion

A. Fabrication

Fig. 5 shows a prototype of the self-propelled robot. Table 2 shows the size of the prototype. Flexible paddles (legs of the centipede robot craft kit manufactured by TAMIYA INC., Japan) are fixed to the spur gears. The flexible paddles that spread the colon wall are made of TPS (Thermoplastic Styrenic Elastomer, AR-760N, hardness A60, ARONKASEI, Japan). In general, the large intestine of humans is approximately 7.5 cm in diameter when inflated [12]. Therefore, according to the required specifications, the diameter of the robot must be ≤26 mm, and by considering the size of the gear and center-to-center distance between two spur gears, the length of the paddle must be ≥30 mm. The length and diameter of the paddle were measured using a caliper. The measured length is 30 mm, which is considered reasonable. The shape of the paddle should deform along the wall of the large intestine. In addition, to ensure compactness of the robot, a thin paddle shape is desired. In this study, we decided to confirm the feasibility of such a shape by designing the paddle with a taper that thins toward the tip. Therefore, the paddles had diameters of 3.5 mm at the proximal end and 2 mm at the tip. The closer to the root portion of the paddle, the larger moment is applied because of the moment arm is longest at the root. Therefore, less rigidity is required at the tip of the paddle than root. This is the reason to employ the taper shape. The gears and case were fabricated using a 3D printer (Objet 500 Connex, Stratasys, U.S.A). The worm gear is fixed at the tip of the torque transmission shaft, which is a flexible shaft (S-325C, Showa spring MFG, Japan) with diameter of 3.0 mm and length of 1 m. A torque-retaining outer tube (liner blade tube, inner and outer diameters of ϕ7.0–8.0 mm, Hagitec, Japan) with heat-shrinkable outer surface is fixed to the robot case and motor base. A flexible shaft is connected to the motor

shaft via a coupling and is rotated by the motor (BMU2600A-AC-1, Oriental motor, Japan). The heat-shrinkable outer surface was made of silicon rubber, whereas the flexible shaft and torque-retaining tube were made of stainless steel. These are generally biocompatible materials. The flexible paddle is selected from available samples close to desired shape. For the gears and case, 3D printer was used because of rapid prototyping in this research. In the future, these will be replaced by biocompatible materials which can be used repeatedly by sterilization.

B. Model Verification

We evaluated the model by comparing the theoretical values with the experimental values obtained with the fabricated prototype.

First, the normal force according to the displacement x was experimentally obtained. The experimental system for force measurement is shown in Fig. 6(a). First, a flexible paddle was fixed to the fixing table. A force gauge (ZTA-5N, IMADA, Japan) was attached to the vertical electric measuring stand (EMX-1000N, IMADA, Japan), and a fixed base was attached to the stage. The force gauge was moved vertically downward at a constant speed of 20 mm/min, and the tip was pressed by the flexible paddle. Using a ruler, the point on which the load was applied to the flexible paddle was shifted by 1 mm (Fig. 6(b)). A connecting rod with a V-shaped tip was attached to prevent interference between the force gauge and the fixing table (Fig. 6 (c)). The experimental value of the normal force N for displacement x is shown in Fig. 7(a).

Next, we calculated the theoretical value of F_p with the experimental value of N. In this study, we used PVC (polyvinyl chloride) phantoms (colonoscopy training model, M40-11361-000, KYOTO KAGAKU, Japan) as models of the large intestine (Fig. 8(a)). The coefficient of dynamic friction of PVC, μ_p, is approximately 0.17 [19], which was selected as a reference value in this study, as it is necessary to depend on both the material in contact and surface condition. The length of the flexible paddle, l, was 30 mm. The center-to-center distance between two spur gears, d, was 15 mm. The diameter of each phantom, W, was measured at the narrowest point of the tract. When there were semilunar folds in the colon, W was measured at their tip. When the friction force between the large intestine wall and sheath F_f is zero, the theoretical propulsive force F_p at each diameter W of the phantom is as shown in Fig. 7(b).

Finally, we obtained the experimental value of F_p. During the experiment, the maximum propulsive force was measured by a force gauge at (A) sigmoid colon, (B) descending colon, (C) ascending colon, and (D) intestinal tract injection port of the phantoms, as shown in Fig. 8(a). When measuring the propulsive force, the motor speed was constant at 500 rpm to maintain the same experimental conditions in different trials. Fig. 8(b) depicts the locomotion in the phantom and Fig. 8(c) shows the experimental setup. The thread connects the force gauge to the back end of the robot. Fig. 7(b) shows the experimental values of the propulsive forces and their comparison with the theoretical values. The following maximum propulsive forces were obtained for each part: (A) 0.39 N, (B) 0.91 N, (C) 0.79 N, and (D) 1.26 N. The experimental values from (A) to (D) were between the values

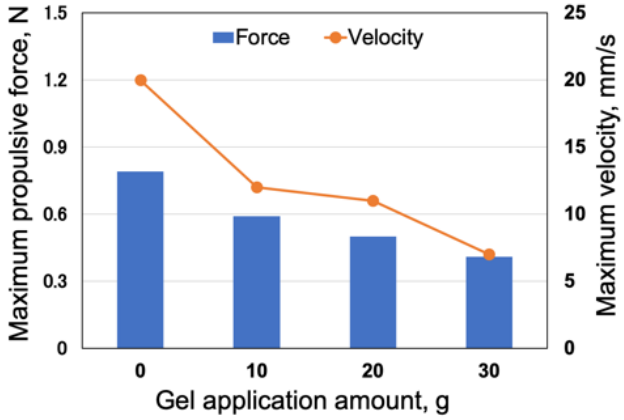

Fig. 9. Experimental results: maximum propulsive force and velocity of locomotion in the phantom for each gel-application amount. (Motor speed: 500 rpm).

of (2) and (3). As shown in Fig. 7(b), the propulsive force was larger in the colon with semilunar folds. The experimental values were shown to be within the theoretical values, and the modeling was confirmed to be valid. In reality, the propulsive force may be larger because of the effect of friction between the thread and phantom. In addition, the velocity and forces may be affected in the case of a phase difference between the two paddles. The phase difference results in a large friction because the robot body contacts the intestinal walls in the opposite side of the paddle. As the propulsive force was about 1 N, it may be possible to satisfy the required specifications with future improvements. In this experiment, the robot operated smoothly without a pause. This could be because the paddles were able to flexibly deform and conform to the shape of the semilunar folds and walls to obtain frictional force. The prototype shown in the paper, could not pass through the curved section like the sigmoid colon, descending-transverse and transverse-ascending junctions.

Next, we examined whether the difference in the friction condition in the phantom influences the maneuverability of the proposed robot. Gel (Gatsby tightening Shaving Gel 205 g, ASIN: B00ST803FC, MANDOM, Japan) was applied to the surface of the phantom to change the friction condition. By using the setup in Fig. 8(c), we tested the prototype with different propulsion forces and velocities, with increase in the amount of applied gel up to 10 g. The maximum velocity was measured from the video. Furthermore, the maximum propulsive force was measured by connecting a force gauge placed on the opposite side of the locomotion direction with a thread tied to the end of the sheath. The maximum propulsive force and velocity of the locomotion experiment in the phantom for each gel application are shown in Fig. 9. We confirmed that the robot could move even if the gel was applied on the internal wall of the phantom. The maximum velocity of the robot was about the same as the required speed of 6.5 mm/s. However, the maximum propulsive force and velocity decreased as the amount of applied gel was increased. This could be because the proposed mechanism uses the frictional force to obtain the propulsive force, and the coefficient of dynamic friction between the flexible paddles and the wall was reduced by the application of the gel.

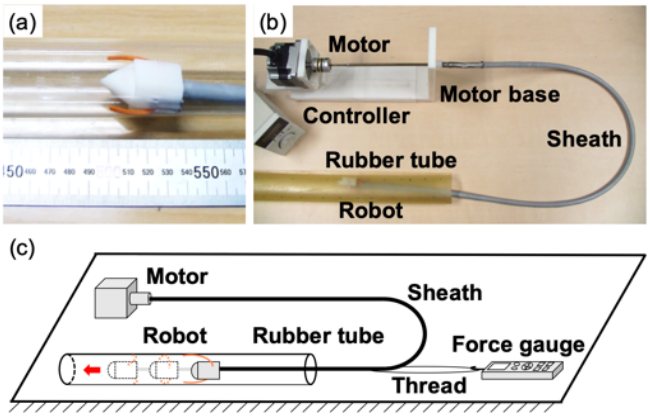

Fig. 10. Overview of the experiments. (a) Image of locomotion in an acrylic pipe. (b) Image of locomotion in a rubber tube. (c) Propulsion force measurement using a force gauge.

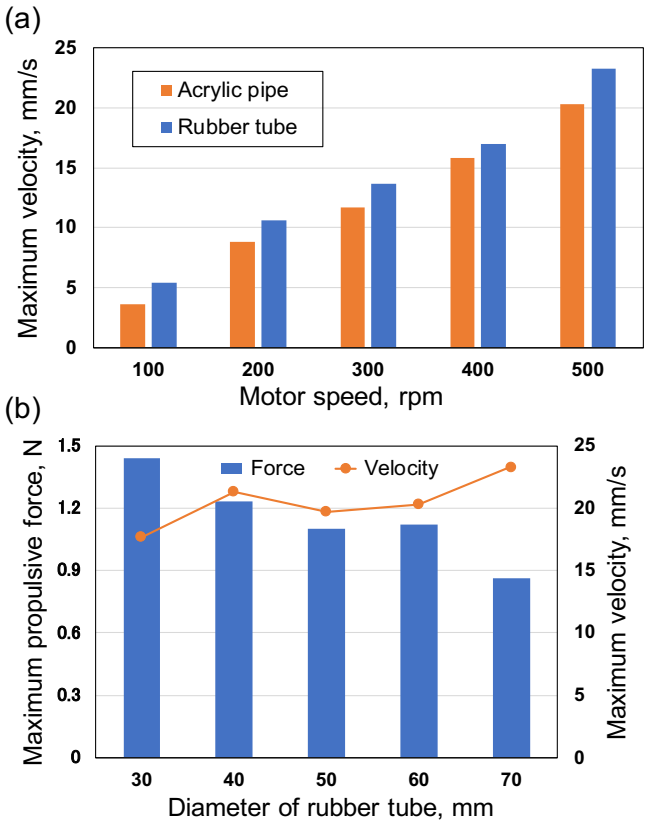

Fig. 11. Experimental results showing (a) maximum velocity of locomotion in acrylic pipe and rubber tube at each motor speed (Tube diameter: 35 mm), and (b) maximum propulsive force and velocity of locomotion in rubber tube for each diameter (Motor speed: 500 rpm).

However, the characteristics of the flexible rubber, such as hardness and surface roughness, have not been examined in detail, which will be studied in the next step of this research work.

C. *Locomotion in the simulated intestinal tract*

The purpose of this experiment was to evaluate whether the developed robot satisfied the required specifications of the self-propelled colonoscopy robot. First, we verified whether it could move forward along the intended path. Because the colonoscopy-training model had a constant inner diameter, we prepared a simulated intestinal tract made of urethane rubber tube (UTSLL 1-500-500, hardness A30, MISUMI, Japan). The diameter of the tube could be easily adjusted. As a preliminary experiment, we also prepared an acrylic pipe (inner and outer diameters of φ35–41 mm). The experiment to verify the locomotion was carried out in a 300-mm length of the tube with inner diameter of 35 mm. The maximum velocity when the paddle was rotated twice was measured from the video. The motor speed was varied at intervals of 100 rpm from 100 to 500 rpm (equivalent speed at the spur gear was approximately 6 to 28 rpm). Fig. 10 shows the experimental system. The maximum velocity of the locomotion in the acrylic pipe and rubber tube are shown in Fig. 11(a). The self-propelled colonoscopy robot moved 300 mm regardless of the pipe hardness. The difference in velocity between the acrylic pipe and rubber intestinal tract was small. When the motor speed was higher than 200 rpm, it was faster than the insertion speed of 6.5 mm/s by an expert.

Next, we verified that sufficient speed and thrust force could be obtained in tubes of different inner diameters. Five types of rubber intestines of 500-mm length were prepared with inner diameters of 30, 40, 50, 60, and 70 mm. The maximum velocity was measured from the video. The maximum propulsive force was measured by connecting a force gauge placed on the opposite side of the locomotion direction with a thread tied to the end of the sheath. The maximum propulsive force and velocity of the locomotion experiment in different diameters of the rubber tube are shown in Fig. 11(b). The robot traversed the rubber tube length of 300 mm in all rubber intestinal tracts of different inner diameters. The velocity of the robot exceeded the speed of 6.5 mm/s. Furthermore, the robot obtained a propulsive force of 1 N or more in tubes with diameter varying between 30 mm and 60 mm. The results reveal that the prototype could cope with the changes in the inner diameter of the large intestine. The propulsive force did not decrease significantly because the rubber tube was pushed by gravitational force. As such, the rubber tube has a smaller vertical inner diameter. This increases the vertical force of the robot as it pushes against the walls. As the propulsive force of the robot is proportional to the normal force, it has a larger value. In current colonoscopy, the diameter of the human colon enlarged by insufflation. Although some results of the propulsive force in the training model are slightly less than 1N according to diameter, we think it is possible to obtain 1N by insufflation control. Thus, the effectiveness of the robot principle is confirmed.

IV. Conclusion

We proposed a novel self-propelled robot using flexible paddles that support the insertion of a colonoscope. In this method, a torque is transmitted from a motor outside the patient body to a worm gear at the tip of the colonoscope by a flexible shaft. The worm gear is engaged with two spur gears, and flexible paddles fixed to these spur gears contact the wall of the large intestine to provide the propulsive force. We created a force transmission model of the robot to confirm the suitability of the design. A prototype of the self-propelled robot was fabricated by a 3D printer, and its locomotion in a simulated rubber intestine was evaluated. The velocity of the robot was faster than the required speed of 6.5 mm/s. The

propulsive force was about 1 N, and thus the effectiveness of the robotic principle was confirmed. The insertion through the curved section like the sigmoid colon, descending-transverse and transverse-ascending junctions is challenging. For this purpose, we think that the active bending section (like standard flexible endoscopes have at the tip) should be implemented to change the direction of the proposed robot so that the robot can avoid heading towards the colon wall at the curved section. In the future study, we would like to implement the active bending section.

The use of flexible paddles for a self-propelled colonoscopy robot is a novel approach. In comparison with the operating mechanisms of other self-propelled robots, this robot has a simpler structure and mechanism. It is composed of a motor base, motor, flexible shaft, a sheath, a worm gear, two spur gears, two flexible paddles, and a case. The notable feature of the proposed mechanism is that the number of mechanical components is greatly reduced when compared with the previously presented mechanism, because of the use of elastic paddles. This greatly contributes to the downsizing of the structure. Consequently, we succeeded in fabricating a compact robot with diameter of 26 mm and length of 40 mm. The mechanical locomotion design, its fabrication, and analysis results reported in this paper are its main contributions. They represent important steps toward the development of a practical clinical self-propelled colonoscopy robot with flexible paddles.

In the future, locomotion evaluation will be performed using porcine colon. Although the colonoscopy-training model used in the experiment faithfully reproduces the structure of the large intestine, the coefficient of kinematic friction is smaller in porcine colon because of its wet surface. The coefficient of dynamic friction μ_p and normal force N should be increased to obtain sufficient propulsive force (cf. (2) and (3)). The following are possible solutions to this problem. (1) A harder rubber can be used for the flexible paddle. (2) The surface of the flexible paddle could be roughened to increase the coefficient of dynamic friction. (3) Protrusions could be introduced on the surface of the flexible paddle to allow it to easily gain friction with the colon wall. (4) The propulsive force may be increased by increasing the number of flexible paddles. For all these methods, the damage to the intestinal wall should be carefully considered. Furthermore, we will investigate the implementation of a bending mechanism, camera, and forceps port.

ACKNOWLEDGEMENTS

We would like to thank Editage (www.editage.com) for English language editing.

REFERENCES

[1] J. S. Moore and T. H. Aulet, "Colorectal cancer screening," *Surg. Clin. North Am.*, vol. 97, no. 3, pp. 487–502, 2017.

[2] G. Iddan, G. Meron, A. Glukhovsky, and P. Swain, "Wireless capsule endoscopy," *Nature*, vol. 405, no. 6785, pp. 417, 2000.

[3] M. Delvaux and G. Gay, "Capsule endoscopy in 2005: Facts and perspectives," *Best Pract. Res. Clin. Gastroenterol.*, vol. 20, no. 1, pp. 23–39, 2006.

[4] E. Morita, N. Ohtsuka, Y. Shindo, S. Nouda, T. Kuramoto, T. Inoue, M. Murano, E. Umegaki, and K. Higuchi, "In vivo trial of a driving system for a self-propelling capsule endoscope using a magnetic field (with video)," *Gastrointest. Endosc.*, vol. 72, no. 4, pp. 836–840, 2010.

[5] G. Pittiglio, L. Barducci, J. W. Martin, J. C. Norton, C. A. Avizzano, K. L. Obstein, and P. Valdastri, "Magnetic Levitation for Soft-Tethered Capsule Colonoscopy Actuated With a Single Permanent Magnet : A Dynamic Control Approach," *IEEE Robot. Autom. Lett.*, vol. 4, no. 2, pp. 1224–1231, 2019.

[6] K. Suzumori, T. Hama, and T. Kanda, "New Pneumatic Rubber Actuators to Assist Colonoscope Insertion," in *Proc. IEEE Int. Conf. Robot. Autom.*, Orlando, FL, 2006, pp. 1824–1829.

[7] G. Trovato, M. Shikanai, G. Ukawa, J. Kinoshita, N. Murai, J. W. Lee, H. Ishii, A. Takanishi, K. Tanoue, S. Ieiri, K. Konishi, and M. Hashizume, "Development of a colon endoscope robot that adjusts its locomotion through the use of reinforcement learning," *Int. J. Comput. Assist. Radiol. Surg.*, vol. 5, no. 4, pp. 317–325, 2010.

[8] A. Eickhoff, R. Jakobs, A. Kamal, S. Mermash, J. F. Riemann, J. Van Dam, "In vitro evaluation of forces exerted by a new computer-assisted colonoscope (the NeoGuide Endoscopy System)," *Endoscopy*, vol. 38, no. 12, pp. 1224–1229, 2006.

[9] J. Bernth, A. Arezzo, and H. Liu, "A Novel Robotic Meshworm With Segment-Bending Anchoring for Colonoscopy," *IEEE Robot. Autom. Lett.*, vol. 2, no. 3, 2017.

[10] H. Kita and H. Yamamoto, "Double-balloon endoscopy for the diagnosis and treatment of small intestinal disease," *Best Pract. Res. Clin. Gastroenterol.*, vol. 20, no. 1, pp. 179–194, 2006.

[11] P. Valdastri, R. J. Webster III, C. Quaglia, M. Quirini, A. Menciassi, and P. Dario, "A new mechanism for mesoscale legged locomotion in compliant tubular environments," *IEEE Trans. Robot.*, vol. 25, no. 5, pp. 1047–1057, 2009.

[12] D. Kim, D. Lee, S. Joe, B. I. Lee, and B. Kim, "The flexible caterpillar based robotic colonoscope actuated by an external motor through a flexible shaft," *J. Mech. Sci. Technol.*, vol. 28, no. 11, pp. 4415–4420, 2014.

[13] A. Alazmani, A. Hood, D. Jayne, A. Neville, and P. Culmer, "Quantitative assessment of colorectal morphology: Implications for robotic colonoscopy," *Med. Eng. Phys.*, vol. 38, no. 2, pp. 148–154, 2016.

[14] J. C. Norton, "The Design and Development of a Mobile Colonoscopy Robot," Ph.D. Thesis, Univ. Leeds, UK, 2017. Available from White Rose eTheses Online (uk.bl.ethos.706010).

[15] I. Kassim, L. Phee, W. S. Ng, F. Gong, P. Dario, and C. A. Mosse, "Locomotion Techniques for Robotic Colonoscopy," *IEEE Eng. Med. Biol. Mag.*, vol. 25, no. 3, pp. 49–56, 2006.

[16] R. E. Sedlack, T. H. Baron, S. M. Downing, and A. J. Schwartz, "Validation of a Colonoscopy Simulation Model for Skills Assessment," *Am. J. Gastroenterol.*, vol. 102, no. 1, pp. 64–74, 2007.

[17] J. Norton, A. Hood, A. Neville, D. Jayne, P. Culmer, A. Alazmani, and J. Boyle, "RollerBall: a mobile robot for intraluminal locomotion," in *Proc. 6th IEEE RAS/EMGS Int. Conf. Biomed. Robot. Biomechatron.*, Singapore, 2016, pp. 254–259.

[18] K. Osawa, R. Nakadate, J. Arata, S. Onogi, T. Akahoshi, Y. Soejima, and M. Hashizume, "Development of a Self-Propelled Colonoscope Robot with a Conical Worm Gear Mechanism," *J. Japan Soc. Comput. Aided Surg.*, vol. 1, no. 1, pp. 5–11, 2019. [in Japanese]

[19] C. Maier and T. Calafut, *Polypropylene: The Definitive User's Guide and Databook*, New York: William Andrew, 1st Ed., 1999, pp. 134.